

Coupling effect of active and reactive power controls on synchronous stability of VSGs

Deng, Han; Fang, Jingyang; Tang, Yi; Debusschere, Vincent

2019

Deng, H., Fang, J., Tang, Y., & Debusschere, V. (2019). Coupling effect of active and reactive power controls on synchronous stability of VSGs. The 4th IEEE International Future Energy Electronics Conference (IFEEEC 2019).

<https://hdl.handle.net/10356/93528>

© 2019 IEEE. Personal use of this material is permitted. Permission from IEEE must be obtained for all other uses, in any current or future media, including reprinting/republishing this material for advertising or promotional purposes, creating new collective works, for resale or redistribution to servers or lists, or reuse of any copyrighted component of this work in other works.

Downloaded on 18 Jan 2022 15:19:02 SGT

Coupling Effect of Active and Reactive Power Controls on Synchronous Stability of VSGs

Deng Han
Energy Research Institute @ NTU
ERI@N
Interdisciplinary Graduate School
Nanyang Technological University
Singapore
E-mail: han017@e.ntu.edu.sg

Jingyang Fang, Yi Tang
School of Electrical and Electronic
Engineering
Nanyang Technological University
Singapore
E-mail: jfang006@e.ntu.edu.sg,
yitang@ntu.edu.sg

Vincent Debusschere
Univ. Grenoble Alpes,
CNRS, Grenoble INP*, G2Elab
38000 Grenoble
France
E-mail:
vincent.debusschere@grenoble-inp.fr

Abstract— The virtual synchronous generator (VSG) is emerging as a promising candidate for replacing synchronous generators in more-electronics power systems. Its fundamental objective lies in the regulation of active and reactive power for voltage forming and frequency control. To achieve tight power regulation, VSGs usually have closed-loop active power and reactive power controls. However, this paper reveals that the coupling effect between the active power control and the reactive power control will greatly change the synchronous stability of a VSG. Specifically, the maximum transferred active power and its associated power angle are reduced because of the coupling effect. To quantify this effect, a small-signal model of a grid-tied VSG is constructed, based on which the critical operation point is further analyzed. The power angle curve of VSGs with fixed reactive power output is compared with that of VSGs with constant output voltage amplitude. Finally, the effect of reactive power droop control in increasing the stable operation region is investigated in this paper.

Keywords—virtual synchronous generator, power regulation, coupling effect, synchronous stability

I. INTRODUCTION

Renewable generation systems are increasingly used in modern power systems to reduce carbon emissions and improve energy sustainability. Typically, grid-tied power converters serve as the interfaces for renewable generation systems, energy storage systems, etc. [1]. The ever-increasing penetration level of power electronic converters reduces the proportion of synchronous generators (SG) in modern power systems. As power converters feature no inertia response, they reduce the inertia level of modern power systems, leading to poor frequency regulation and even grid failures. [2].

To better integrate renewables, grid friendly converters are proposed as an effective solution for providing distributed virtual inertia and increasing the inertia level of more-electronics power systems [2]. Grid friendly converters can be generally classified into two types – grid-feeding converters which are controlled as ac current sources and grid forming converters which are controlled as ac voltage sources [3]. Specifically, grid-feeding converters simply regulate their output currents or power and follow the grid without regulating the grid voltages. In contrast, grid-forming converters regulate voltages and frequency. Grid-forming converters can also transmit seamlessly between the grid-connected (GC) mode and standalone (SA) mode. Under weak grid conditions, voltage controlled converters can provide direct voltage support as SGs do. The self-synchronize

characteristic of grid-forming converters makes phase-locked loops not necessarily required for them [4]. Besides, in power electronics dominated power systems, voltage controlled converters are indispensable for forming the grid voltages. The similarities between grid-forming converters and SGs make grid-forming converters more suitable than grid-feeding converters in more-electronics power systems.

VSGs (or VSMs, VISMAAs [5], synchronverters [6], static SGs [7]) were proposed to emulate SGs behaviors such as inertia response, damping, droop mechanism and excitation regulators with grid-forming converters. They can provide grid support by adapting their active and reactive power output according to the amplitude and frequency of the grid voltage. Like SGs, VSGs usually tune their speed or their phase angle difference with the grid and their voltage amplitude at the point of common coupling (PCC) to regulate their power output [4]. When the transmission line impedance is inductive, the active power is controlled by the power angle and the reactive power is controlled by the voltage amplitude. Closed-loop control is usually employed to eliminate the steady state error between the output power and the power reference. However, the regulation of active power and reactive power is not independent. The coupling effect between active and reactive power controls makes the controller design complicated [8]. In addition, power loops gains are also affected because of the coupling effect.

This paper builds a multiple-input-multiple-output (MIMO) model of a grid-tied VSG. The VSG is controlled to output the desired power without any error. The analysis of this model shows that the active power loop gain becomes negative before the power angle reaches 90° , which is the maximum theoretical power angle for synchronous stability [9] of a fixed voltage amplitude VSG in steady state. The power-angle curve is further plotted, showing that the maximum transferred power is also reduced as compared with a fixed voltage amplitude VSG.

Another problem introduced by the closed-loop power control is that the voltage amplitude will deviate a lot from the rated value. Since only two among power angle, voltage amplitude, active power and reactive power of a VSG are independent. To enlarge the maximum transferred active power and make a compromise between the VSG voltage and the reactive power, the reactive power droop control is also studied in this paper. It should be noted that, in some research works, grid side voltage amplitudes are detected to implement reactive power droop control [4], while in others, VSG voltage amplitudes are used [8]. Usually, droop control with the grid side voltage amplitude aims at providing voltage support and

* Institute of Engineering Univ. Grenoble Alpes

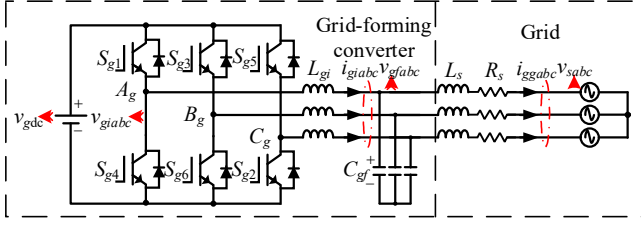


Fig. 1. Schematic diagram of a grid-tied VSG.

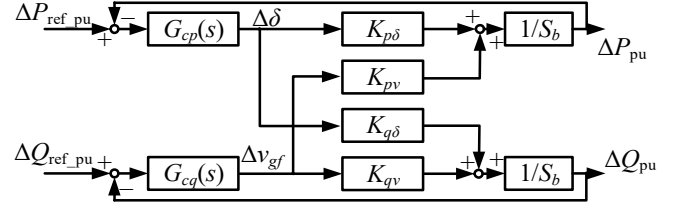


Fig. 2. Small signal model of the VSG.

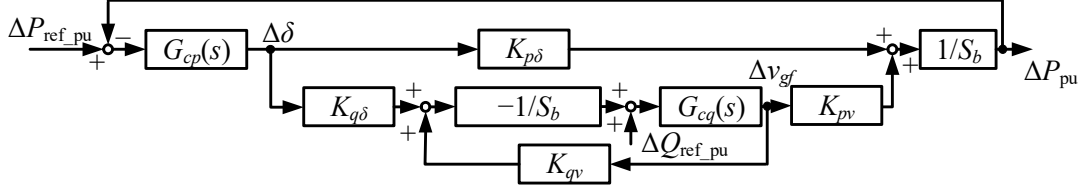


Fig. 3. Reorganized small signal model of VSG.

achieving reactive power sharing when grid voltage varies, and reactive power droop control at VSG side intends to keep the VSG voltage amplitude within a certain range. This paper only considers the reactive power droop control at VSG side.

II. COUPLING EFFECT ANALYSIS

A. Model of a Grid-Tied VSG

Fig. 1 shows the schematic diagram of a grid-tied VSG, where a DC-AC inverter is connected to the grid through an LC filter. The system can be considered as a simple 2-machine system, in which the VSG rms phase voltage and grid rms phase voltage are V_{gf} and V_s , respectively, and their nominal value is V_n . The active power P and the reactive power Q on the VSG side can be calculated as:

$$P + jQ = 3\dot{V}_{gf} \dot{I}_{gg}^* = 3V_{gf} \angle \delta_0 \cdot \left(\frac{V_{gf} \angle \delta_0 - V_s \angle 0}{R_s + jX_s} \right)^* \quad (1)$$

$$P = \frac{3V_{gf} (V_{gf} R_s - V_s R_s \cos \delta_0 + V_s X_s \sin \delta_0)}{R_s^2 + X_s^2} \quad (2)$$

$$Q = \frac{3V_{gf} (V_{gf} X_s - V_s X_s \cos \delta_0 - V_s R_s \sin \delta_0)}{R_s^2 + X_s^2} \quad (3)$$

where δ_0 is the power angle between the VSG voltage and the grid voltage, R_s and jX_s are the resistive and the inductive parts of the line impedance, respectively. In this paper, the line is considered inductive, i.e. $R_s \ll X_s$. P and Q can be considered as binary functions of δ_0 and V_{gf} . To linearize the functions, the quasi-static relationship of P , Q and δ_0 , V_{gf} is achieved by taking the partial derivatives of (2) and (3) with respect to δ_0 and V_{gf} :

$$K_{p\delta} = \frac{\partial P}{\partial \delta} = \frac{3V_{gf} V_s (R_s \sin \delta_0 + X_s \cos \delta_0)}{R_s^2 + X_s^2} \quad (4)$$

$$K_{pv} = \frac{\partial P}{\partial v_{gf}} = \frac{3(2V_{gf} R_s + V_s (-R_s \cos \delta_0 + X_s \sin \delta_0))}{R_s^2 + X_s^2} \quad (5)$$

$$K_{q\delta} = \frac{\partial Q}{\partial \delta} = \frac{3V_{gf} V_s (-R_s \cos \delta_0 + X_s \sin \delta_0)}{R_s^2 + X_s^2} \quad (6)$$

$$K_{qv} = \frac{\partial Q}{\partial v_{gf}} = \frac{3(2V_{gf} X_s + V_s (-R_s \sin \delta_0 - X_s \cos \delta_0))}{R_s^2 + X_s^2} \quad (7)$$

where $K_{p\delta}$, K_{pv} , $K_{q\delta}$ and K_{qv} are the partial differentials of P and Q . According to (4)-(7), the minor change in P and Q can be represented by:

$$\Delta P_{pu} = (K_{p\delta} \Delta \delta + K_{pv} \Delta v_{gf}) / S_b \quad (8)$$

$$\Delta Q_{pu} = (K_{q\delta} \Delta \delta + K_{qv} \Delta v_{gf}) / S_b \quad (9)$$

where Δ denotes a small perturbation.

Like SGs, VSGs tune δ_0 and V_{gf} to control P and Q respectively when the line impedance is inductive. Generally, the small signal model of a VSG can be depicted as Fig. 2 according to (8) and (9), where $G_{cp}(s)$ and $G_{cq}(s)$ are the active and reactive power controllers, respectively, notation 'ref' denotes reference, notation 'pu' means per unit value, and the power base is $S_b = 3V_n^2 / X_s$. VSGs are usually controlled to output a certain value of power, P_{ref_pu} and Q_{ref_pu} are the reference values of the VSG. The inner loop dynamics of voltage and current control are not shown in this model as the inner loop response is considered much faster than the power control loop. To better analyze the active power control loop, Fig. 2 can be reorganized as Fig. 3.

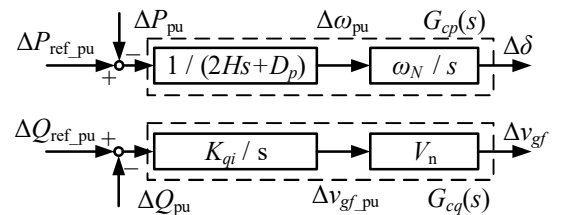


Fig. 4. Active and reactive power controllers.

A basic controller design is shown in Fig. 4, where ω_{pu} is the per unit frequency, ω_n is the nominal value of the grid frequency, H is the virtual inertia constant, D_p is the active power damping coefficient and K_{qi} is the integrator gain of the reactive power controller.

With the integrators in each controller, there will be no steady state error between the output power and the reference.

B. Coupling analysis of the VSG model

If the reactive power reference Q_{ref_pu} is a fixed value, i.e. $\Delta Q_{ref_pu} = 0$, then the open loop transfer function from $\Delta \delta$ to ΔP_{pu} can be calculated from Fig. 3,

$$G_{cp\delta}(s) = \frac{\Delta P_{pu}(s)}{\Delta \delta(s)} = (K_{p\delta} - K_{q\delta} \frac{G_{cq}(s)}{S_b + K_{qv} G_{cq}(s)} K_{pv}) / S_b \quad (10)$$

substituting $G_{cq}(s)$ in Fig. 4 into (10),

$$G_{cp\delta}(s) = \frac{\Delta P_{pu}(s)}{\Delta \delta(s)} = (K_{p\delta} - K_{q\delta} \frac{K_{qi} V_n}{S_b s + K_{qv} K_{qi} V_n} K_{pv}) / S_b \quad (11)$$

At steady state, i.e. $s = 0$,

$$G_{cp\delta}(0) = \Delta P_{pu} / \Delta \delta = (K_{p\delta} - K_{q\delta} K_{pv} / K_{qv}) / S_b \quad (12)$$

To control ΔP_{pu} with $\Delta \delta$, (12) should always have the same sign so negative feedback always stands. The solution of

$$K_{p\delta} - K_{q\delta} K_{pv} / K_{qv} = 0 \quad (13)$$

is

$$\delta_0 = \pm \arccos\left(\frac{V_s}{2V_{gf}}\right) = \pm \delta_{max} \quad (14)$$

If the power angle is within $[-\delta_{max}, \delta_{max}]$, the system can be controlled without change of the controller, or the system has a stable equilibrium point. However, if the power angle exceeds the range, the sign of the power loop gain changes and the negative feedback becomes positive feedback, then the system is no longer stable with the original controller.

To illustrate, when $R_s \ll X_s$, (2) becomes

$$P = \frac{3V_{gf} V_s \sin \delta_0}{X_s} \quad (15)$$

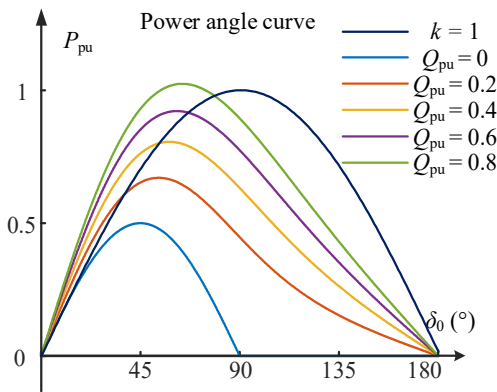


Fig. 5. Power angle curves under different reactive power output.

and with fixed voltage control, (8) becomes

$$\Delta P_{pu} = \frac{3V_{gf} V_s \cos \delta_0}{X_s S_b} \Delta \delta \quad (16)$$

when $\delta_0 \in [-\pi/2, \pi/2]$, the system is synchronous stable. However, when the VSG reactive power is controlled at a fixed value, only when

$$\delta_0 \in \left[-\arccos\left(\frac{V_s}{2V_{gf}}\right), \arccos\left(\frac{V_s}{2V_{gf}}\right) \right] \quad (17)$$

the VSG is synchronous stable. As $V_s / 2V_{gf} > 0$ always stands in normal conditions, the maximum power angle will not reach $\pi/2$ as the fixed voltage control.

C. Power angle curve of P and Q control

The change of the maximum power angle for synchronous stability can be further illustrated by plotting the power angle curve of a fixed reactive power controlled VSG system according to (2) and (3). This paper assumes $V_s = V_n$ and defines $k = V_{gf} / V_s$, and the power base is $S_b = 3V_n^2 / X_s$. Then equations (2) and (3) become

$$P_{pu} = k \sin \delta_0 \quad (18)$$

$$Q_{pu} = k(k - \cos \delta_0) \quad (19)$$

When the VSG is under fixed reactive power control, k can be solved from (19)

$$k = \frac{\cos \delta_0 \pm \sqrt{\cos^2 \delta_0 + 4Q_{pu}}}{2} \quad (20)$$

as there are two solutions in (20), the larger k is chosen to maintain continuousness. The relationship between the power angle and the active power can be further calculated by substituting (20) into (18).

Fig. 5 shows the power angle curve. Specially, when Q_{pu} is controlled at 0, the maximum power angle becomes $\pi/4$ and the maximum transferred power becomes 0.5, which reduces a half compared with fixed voltage control, i.e. $k = 1$. Increasing Q_{pu} will increase the maximum synchronous stable power angle and the maximum transferred active power, but high reactive power is not desirable as it will cause high transmission power loss and limit the transferred active

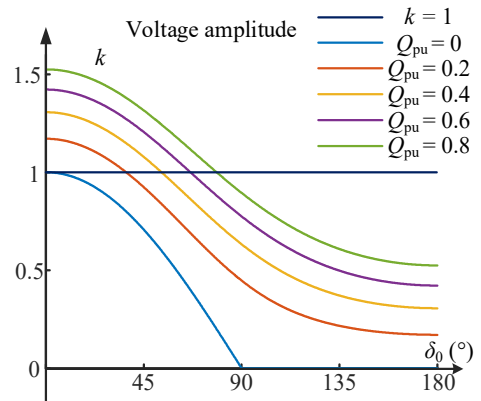


Fig. 6. VSG voltage amplitude under different reactive power output.

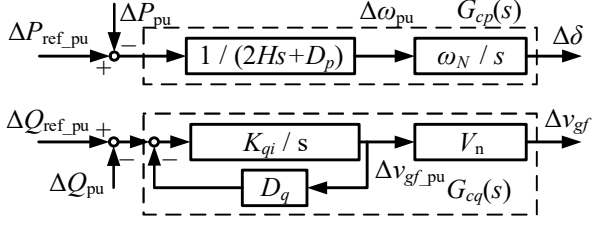


Fig. 7. Power controllers under reactive power droop control.

power. As presented in Fig. 5, to achieve a similar maximum transferred active power as fixed voltage control, Q_{pu} should be over 0.6, while the power factor will be small by then.

Besides, the P and Q control will also make the VSG voltage amplitude out of the desired range. The voltage amplitudes under different reactive power outputs are shown in Fig. 6. With a fixed reactive power output, the VSG voltage diverges a lot at large power angle, which exceeds $\pm 10\%$ of the nominal voltage.

III. DROOP CONTROL ANALYSIS

A. Reactive power droop control analysis

For a grid-tied VSG, only two variables among active power P , reactive power Q , power angle δ and voltage amplitude V_{gf} are independent as the four variables are limited by (2) and (3). Sometimes the VSGs are required to limit their voltage amplitude within a certain range, i.e. $\pm 10\%$ of the nominal value. As shown in Fig. 6, the fixed reactive power control may change the VSG side voltage greatly when the power angle is large. To make a compromise between voltage and reactive power, droop control is usually employed in VSG control.

The block diagram of the reactive power droop controller is presented in Fig. 6. With reactive power droop control, the reactive power output is no longer the same as the reactive power set value, the deviation of the VSG voltage amplitude is translated into additional reactive power,

$$Q_{\text{droop_pu}} = -(1-k)D_q \quad (21)$$

In this paper, only droop in VSG side is considered.

When reactive power reference is fixed, i.e. $\Delta Q_{\text{ref_pu}} = 0$, the quasi-static open loop transfer function from power angle $\Delta\delta$ to active power output ΔP_{pu} in Fig. 3 becomes:

$$G_{cp\delta}(s) = \frac{\Delta P_{pu}(s)}{\Delta\delta(s)} = (K_{p\delta} - K_{q\delta} \frac{K_{qi}V_n}{S_b S + S_b D_q K_{qi} + K_{qv} K_{qi} V_n} K_{pv}) / S_b \quad (22)$$

At steady state, i.e. $s = 0$, the open loop gain becomes

$$G_{cp\delta}(0) = \Delta P_{pu} / \Delta\delta = (K_{p\delta} - \frac{K_{q\delta} V_n K_{pv}}{S_b D_q + K_{qv} V_n}) / S_b \quad (23)$$

When the grid voltage amplitude V_s is equal to the nominal voltage V_n , the solution of

$$K_{p\delta} - \frac{K_{q\delta} V_n K_{pv}}{S_b D_q + K_{qv} V_n} = 0 \quad (24)$$

is

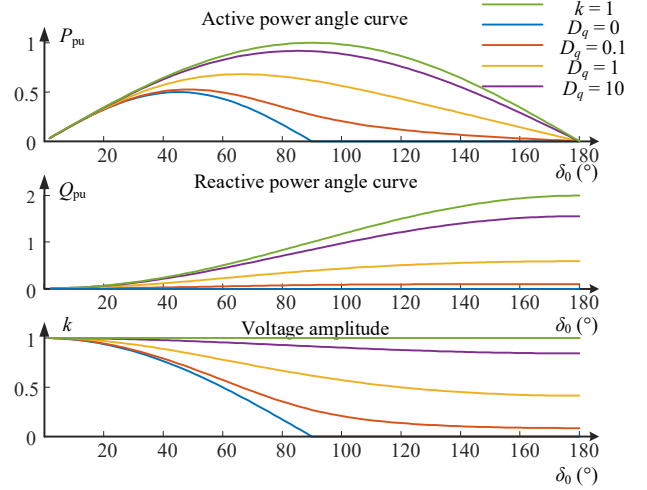


Fig. 8. P_{pu} , Q_{pu} and k under reactive power droop control.

$$\delta_0 = \pm \arccos\left(\frac{V_s}{2(V_{gf} + D_q V_s)}\right) = \pm \delta_{\text{max_D}} \quad (25)$$

Compared with (14), $\delta_{\text{max_D}}$ is larger than δ_{max} , so the synchronous stability range of power angle is extended by the reactive power droop control.

B. Power angle curve of reactive power droop control

Assuming $V_s = V_n$ and $k = V_{gf} / V_s$ and defining the droop reactive power reference as $Q_{\text{droop_pu}} = -(1-k)D_q$, then at steady state, $Q_{pu} = -Q_{\text{droop_pu}}$. With this relationship, (19) can be solved according to the value of D_q ,

$$k = \frac{\cos \delta_0 - D_q \pm \sqrt{(\cos \delta_0 - D_q)^2 + 4D_q}}{2} \quad (26)$$

To ensure continuity, the larger solution is chosen. The active power and reactive power can be further calculated by replacing k in (18) and (19) with (26). Fig. 8 plots the active power P_{pu} , reactive power Q_{pu} and VSG voltage amplitude k at different power angle δ_0 under different D_q . A larger D_q results in a smaller change in voltage amplitude and higher maximum transferred active power, while the reactive power is no longer the same as the set value, and the larger D_q results in the larger difference.

C. Active power droop control

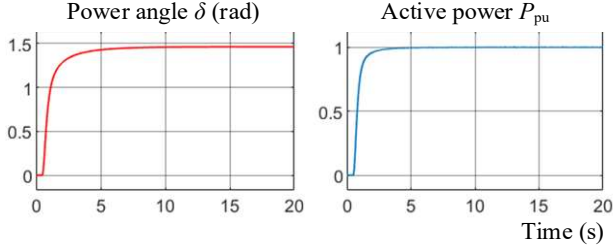
Active power droop control translates the frequency deviation into the active power output,

$$P_{\text{droop_pu}} = -D_{\text{droop_p}}(\omega_{pu} - 1) \quad (27)$$

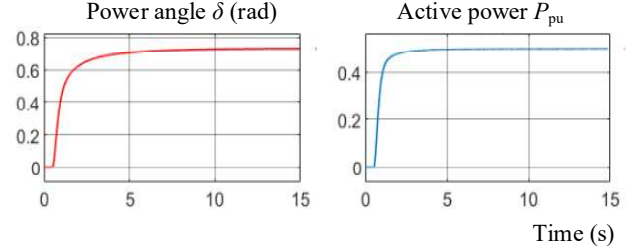
while the steady state frequency of a grid-tied VSG is the same as the grid frequency [4]. In this paper, the grid is considered as a stiff grid with constant frequency, so active power droop control is not considered.

IV. SIMULATION RESULTS

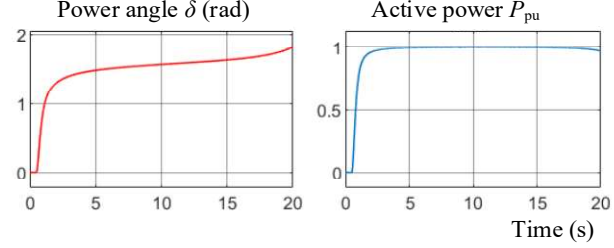
Simulations were carried out under the Matlab/Simulink environment, where the system parameters and control parameters are listed in TABLE I and TABLE II, respectively. The simulation results are shown in Fig. 9 to Fig. 11.



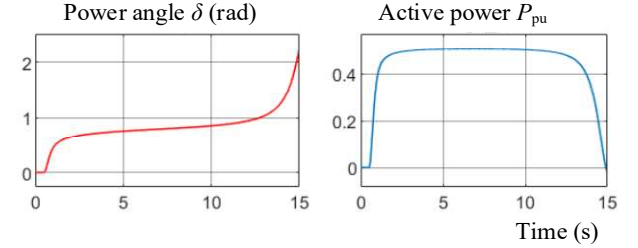
(a) $P_{\text{ref_pu}}$ steps from 0 to 1



(a) $P_{\text{ref_pu}}$ steps from 0 to 0.5



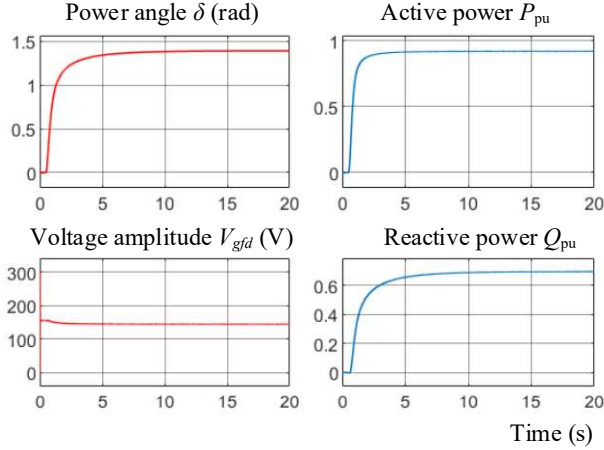
(b) $P_{\text{ref_pu}}$ steps from 0 to 1.01



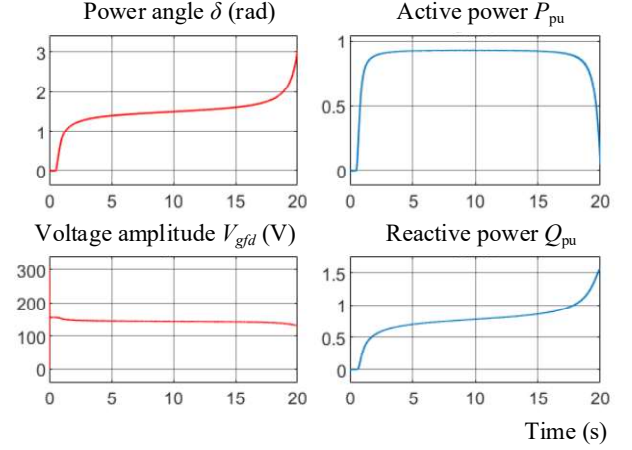
(b) $P_{\text{ref_pu}}$ steps from 0 to 0.51

Fig. 9. Power angle and active power at fixed voltage control.

Fig. 10. Power angle and active power when reactive power preset value is 0 pu.



(a) $P_{\text{ref_pu}}$ steps from 0 to 0.92



(b) $P_{\text{ref_pu}}$ steps from 0 to 0.93

Fig. 11. Power angle, active power, voltage amplitude and reactive power dynamic response under the reactive power droop control.

TABLE I. System Parameters.

Description	System Parameter	
	Symbol	Value
Nominal frequency	f_n	50 Hz
Nominal rms phase voltage	V_n	110 V
Grid rms phase voltage	V_s	110 V
LC filter converter side inductance	L_{gi}	2 mH
LC filter capacitance	C_{gf}	40 μ F
Grid resistance	R_s	0 Ω
Grid inductance	L_s	5 mH
DC link voltage	V_{dc}	500 V
Base apparent power	S_b	$\frac{3V_n^2}{2\pi f_n L_s}$

TABLE II. Control Parameters.

Description	Control Parameter	
	Symbol	Value
Sampling rate	f_n	10 kHz
Inertia constant	H	5 s
Damping constant	D_p	100
Reactive power integral gain	K_{qi}	10
Current controller proportional gain	K_{cp}	0.4
Current controller integral gain	K_{ci}	0
Current controller feedback gain	K_{id}	1.6
Voltage controller proportional gain	K_{vp}	0.2
Voltage controller integral gain	K_{vi}	70

Fig. 9 shows when the VSG is under fixed voltage control, the maximum transferred active power is 1 pu, and the maximum synchronous stable power angle is 90° . When the power angle exceeds 90° , increasing power angle will reduce

the active power output, then the system loses synchronous stability.

In Fig. 10, the VSG is controlled to output the preset power value, and the reactive power reference is 0 pu. The maximum transferred active power is reduced to 0.5 pu, and the maximum synchronous stable power angle is 45° . When

the power angle is less than 45° , the larger power angle results in larger active power. When the power angle is larger than 45° , the active power decreases with the growth of the power angle.

If reactive power droop control is applied, the maximum transferred active power and the maximum synchronous stable power angle are increased. Assuming $D_q = 10$ pu, then the corresponding maximum power angle and the transferred active power can be solved with (18), (19) and (25), i.e.

$$k_{10} = 0.92$$

$$\delta_{10} = 87.4^\circ$$

$$P_{10} = 0.92$$

The active power reference step-up response of the active power, the reactive power, the power angle and the voltage amplitude dynamic response is shown in Fig. 11. It is revealed that when the active power set value exceeds the maximum transferred value δ_{10} , the system becomes unstable and the VSG loses the synchronous stability. The reactive power droop control enlarges the maximum transferred active power and reduces the voltage variation, while the reactive power may deviate a lot from the set value as the droop coefficient D_q increases.

V. CONCLUSION

This paper constructs the small-signal model of grid-tied VSGs and analyzes the coupling effect between active and reactive power control loops. It is found that the VSG system will be stable only when the power angle δ_0 , VSG voltage amplitude V_{gf} and grid voltage amplitude V_s satisfy $|\delta_0| \leq \arccos(0.5V_s / V_{gf})$. In addition, the power-angle curves for the VSG systems with reactive power control and voltage amplitude control differ greatly. To be specific, regulation of the reactive power as zero translates into a 50% reduction of active power transfer and its corresponding power angle as compared with the case of voltage amplitude control. Besides, the VSG voltage amplitude also deviates a lot from its nominal value. To further increase the operation region and make a compromise between voltage amplitude and reactive power output, reactive power droop control is analyzed. With reactive power droop control, the VSG will no longer output set value of reactive power, while the maximum transferred active power is enlarged and the VSG voltage amplitude deviates less from the nominal value.

Through the reactive power droop control, the VSG system can provide active power support stably even under large disturbances.

REFERENCES

- [1] F. Blaabjerg, R. Teodorescu, M. Liserre, and A. V. Timbus, "Overview of Control and Grid Synchronization for Distributed Power Generation Systems," *IEEE Transactions on Industrial Electronics*, vol. 53, no. 5, pp. 1398-1409, 2006.
- [2] J. Fang, H. Li, Y. Tang, and F. Blaabjerg, "On the Inertia of Future More-Electronics Power Systems," *IEEE Journal of Emerging and Selected Topics in Power Electronics*, pp. 1-1, 2018.
- [3] J. Rocabert, A. Luna, F. Blaabjerg, and P. Rodríguez, "Control of Power Converters in AC Microgrids," *IEEE Transactions on Power Electronics*, vol. 27, no. 11, pp. 4734-4749, 2012.
- [4] Z. Qing-Chang, N. Phi-Long, M. Zhenyu, and S. Wanxing, "Self-Synchronized Synchronverters: Inverters Without a Dedicated Synchronization Unit," *IEEE Transactions on Power Electronics*, vol. 29, no. 2, pp. 617-630, 2014.
- [5] H. Beck and R. Hesse, "Virtual synchronous machine," in *2007 9th International Conference on Electrical Power Quality and Utilisation*, 2007, pp. 1-6.
- [6] Q.-C. Zhong and G. Weiss, "Synchronverters: Inverters That Mimic Synchronous Generators," *IEEE Transactions on Industrial Electronics*, vol. 58, no. 4, pp. 1259-1267, 2011.
- [7] A. A. Edris *et al.*, "Proposed terms and definitions for flexible ac transmission system (FACTS)," (in English), *IEEE Transactions on Power Delivery*, Article vol. 12, no. 4, pp. 1848-1853, Oct 1997.
- [8] H. Wu *et al.*, "Small-Signal Modeling and Parameters Design for Virtual Synchronous Generators," *IEEE Transactions on Industrial Electronics*, vol. 63, no. 7, pp. 4292-4303, 2016.
- [9] P. Kundur, *Power system stability and control*. McGraw-hill New York, 1994.